NIKHEF PROJECT PLAN: CRYOLINKS
Cryogenic vacuum links to isolate interferometer arms for Advanced Virgo

Physics Motivation

J.F.J. van den Brand[1],
[1] *Nikhef, National Institute for Subatomic Physics,*
P.O. Box 41882, Amsterdam, the Netherlands

May 5, 2011

email address: jo@nikhef.nl

Procedure start date	01/10/2009
Procedure end date	01/10/2013
Document version	v01r01
Version date	05/05/2011

Abstract

The current Virgo vacuum level needs to be improved by about a factor of hundred in order to be compliant with the required Advanced Virgo sensitivity. Such an improvement requires baking out the interferometer arms. To separate these arms from the towers that hold the mirrors and allow the bake-out, four cryogenic vacuum links will be installed. This document describes the scientific motivation for the project.

Contents

1 Introduction

The enhancement of the Virgo sensitivity by a factor of 10 requires an improvement of the present vacuum level to lower the phase noise for YAG light scattering from the residual gas inside the 3 km long interferometer (ITF) arms. At present the system operates at about 10^{-7} mbar (dominated by water) although it has been designed and tested to reach a base pressure below 10^{-9} mbar (dominated by hydrogen) after an overall bakeout. A typical spectrum of gases recently taken in the Virgo West arm is reported in Fig. 1. The lowest point of the

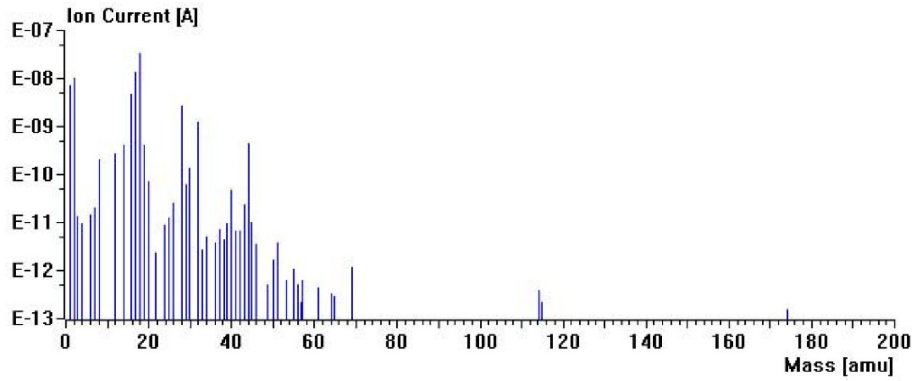

Figure 1: *A recent measurement of the residual gas composition in the West-arm. The horizontal axis reports the ratio mass/charge of the ions and the vertical axis the corresponding ionization current which is proportional to the partial pressure. The dominant peak is the one at mass 18, water. Total pressure is about* 10^{-7} *mbar.*

Advanced Virgo (AdV) sensitivity curve: $3 \times 10^{-24}/\sqrt{\text{Hz}}$ at 200 - 400 Hz is not compatible with the present residual gas phase noise, as shown by Fig. 2. Taking into account all the main species composing the residual gas at the presently attained pressure, the corresponding noise is at the level of $10^{-23}/\sqrt{\text{Hz}}$. To be compatible with the requirements for AdV, this noise has to be reduced by at least a factor of 10 (about a factor of three below the AdV design sensitivity). The residual pressure in the ITF arms has to be reduced by a factor of 100, since the noise is proportional to the square root of the partial pressure of the various gas species (see below).

The selected technique to meet the proposed goal is:

- installing cryogenic links at the interferometer arm extremities;
- performing a bake-out of the ITF arms only.

Cryogenic links are the classical solution to stop the migration of water from unbaked towers to the ITF arms. In the present Virgo configuration, during the restart procedure after opening the towers to service mirrors or suspension systems, the gas released from these towers (mostly water vapor) spreads in the ITF arms, bringing temporarily the residual pressure near 10^{-6} mbar, orders of magnitude above our goal.

Virgo has already experimented with cryolinks, while also LIGO has cryolinks installed on their interferometer. Therefore, we aim at installing cryolinks in Advanced Virgo without a long phase of tests and prototypes. The baking system is already implemented in Virgo, tested and working, hence it will not be discussed here. The expected performance of the cryolinks, after bake-out

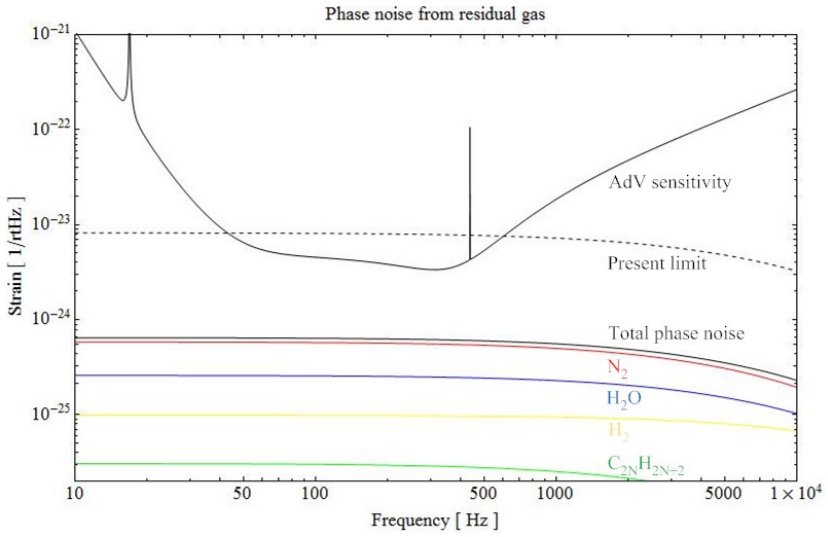

Figure 2: *Advanced Virgo sensitivity curve (purple), phase noise contribution as it would be with the present vacuum level, due to water at a partial presure of* 1.5×10^{-7} *mbar (dashed curve). The sensitivity would be limited to about* $10^{-23}/\sqrt{\text{Hz}}$*. The green, yellow, blue and red curves represent the phase noise due to hydrocarbons, hydrogen, water vapor and nitrogen, respectively. Partial pressures are given in Table 1.1. The solid black curve shows the total expected contribution of phase noise that can be obtained with the cryolinks.*

of the ITF arms, is shown in Table 1, where the contributions of the different gases are reported separately.

Table 1.1. *Proposed goal for phase noise (baked ITF arms) in the 200 - 400 Hz frequency band.*

Gas species	Pressure [mbar]	Noise [$\sqrt{\text{Hz}}$]
Hydrogen	1×10^{-9}	9.7×10^{-26}
Water	1.5×10^{-10}	2.5×10^{-25}
Air	5×10^{-10}	5.6×10^{-25}
Hydrocarbons	1×10^{-13}	2.9×10^{-26}
Total	1.7×10^{-9}	6.2×10^{-25}

2 Phase noise model

The noise is caused by phase fluctuations due to scattering of the laser beam (YAG with a wavelength of 1.064 μm) from background gas. Assuming a gaussian beam and weak scattering the power spectral density of the optical pathlength is given by [1, 2]

$$S_L(f) = \frac{4\rho\,(2\pi\alpha)^2}{v_0} \int_0^{L_0} \frac{1}{w(z)} e^{-2\pi f w(z)/v_0} dz, \tag{1}$$

where the integral is over the beam axis and cavity length L_0. Note that the finesse $\mathcal{F}$ is not contained in this expression, since the photons during their lifetime probe the same scattering centers in the cavity and hence the phase noise from different bounces adds coherently. The parameters are defined as follows:

$w(z)$ Beam radius. For a gaussian beam it is given by

$$w(z) = w_0\sqrt{1 + \frac{(z - z_0)^2}{z_R^2}}, \tag{2}$$

where w_0 is the waist, z_R the Rayleigh range (213 m for AdV) and z_0 the waist position along the axis. For AdV the beam waist will be 8.5 mm and is located at 1385 m from the input mirror. The beam radius on the input mirror (radius of curvature $R_{\mathrm{IM}} = 1416$ m) will be 56 mm and on the output mirror ($R_{\mathrm{EM}} = 1646$ m) is 65 mm.

v_0 Most probable speed of the molecular species. It is given by

$$v_0 = \sqrt{\frac{2k_BT}{m}}, \tag{3}$$

where m is the molecular mass. The Boltzmann constant is represented by k_B and the temperature by T. For room temperature (300 K) we find $v_{\mathrm{N_2}} = 422$ m/s and $v_{\mathrm{H_2O}} = 526$ m/s.

α Molecular polarizability of the gas. The polarizability for nitrogen is $\alpha(\mathrm{N_2}) = 1.6 \times 10^{-24}$ cm^3. Note that the Lorenz-Lorentz relation

$$\frac{4\pi}{3}\sum_A \rho_A\alpha_A = \frac{n^2 - 1}{n^2 + 2}, \tag{4}$$

connects the refraction index and density fluctuations via

$$\frac{4\pi}{3}\sum_A \delta\rho_A\alpha_A = \frac{6\overline{n}}{\left(\overline{n}^2 + 2\right)^2}\delta n \approx \frac{2}{3}\delta n. \tag{5}$$

The molecular polarizability is best derived [1] from measurements of the refractive index of the gas, n, at wavelength $\lambda = 1064$ nm,

$$\alpha(\lambda) = \frac{n(\lambda) - 1}{2\pi\rho_\#}, \tag{6}$$

where $\rho_\# = \frac{N_AP}{RT}$ is the number density of the gas (# molecules/m^3) with $R = 0.06236$ m^3/(Torr mol K) and $N_A = 6.022 \times 10^{23}$ #/mol. At 1 atm and room temperature $\rho_\# \approx 2.4 \times 10^{19}$/cm^3. The molar refractivity measures the polarizability per mol and is given by $A = \frac{4\pi}{3}N_A\alpha$ in cgs units. The molar refractivity remains remarkably constant as the density or pressure is varied, even when there is a change of state. It holds as well for mixtures, when the separate values of A are weighted by the relative number of molecules. For water it amounts to $A_{\mathrm{H_2O}} = 3.71$, while for nitrogen we have $A_{\mathrm{N_2}} = 4.37$. The atomic refractivity of oxygen is 2.01, hydrogen 1.02, carbon 2.11, sulphur 8.23 and chlorine 5.72, so the molar refractivities of many organic compounds can be estimated.

LIGO has experimentally validated Eq. (1) (see ref. [2]). It is based on the following assumptions:

- collisions between molecules are not important (the mean free path for water molecules amounts to $\lambda = xxx$ at a pressure of 10^{-7} mbar);

- a molecule emerges after a collision with the beam pipe with a Boltzmann distribution for its velocity;
- only forward scattering of light is taken into account.

The transversal motion of molecules through the gaussian beam profile leads to a pulse-like dependence of the phase noise. The exponent in Eq. (1) corresponds to the Fourier transform of this pulse shape. The exponential cut in the integral is effective for frequencies greater than the inverse of the typical time needed by a molecule of a given species to travel the distance $2\pi w(z)$. The cut-off frequency is typically in the kHz region (see the curve for the contribution from excess gas in Fig. 2).

The ITF measures the difference in lengths of the two arms and this will have amplitude spectral function $\Delta\tilde{L}(f) \equiv \sqrt{S_{\Delta L(f)}} = \sqrt{2S_L(f)}$. Note that the amplitude spectral density of the pathlength is given by

$$S_L(f) = \left(\frac{dS_L(f)}{d\phi}\right) S_\phi(f), \tag{7}$$

where $S_\phi(f)$ is the phase noise. The phase noise $\Delta\phi$ is related to the length noise by $\Delta l = \frac{\lambda}{2\pi}\Delta\phi$.

For a realistic situation, a sum needs to be taken over all the molecular species present inside the beam pipe. Pressure gradients along the beam pipe are small, but it is possible to take them explicitely into account through integration. Also the beam waist changes in the cavity (see Fig. 3) and its variation should be included in the integration. The diameters of the beam at the

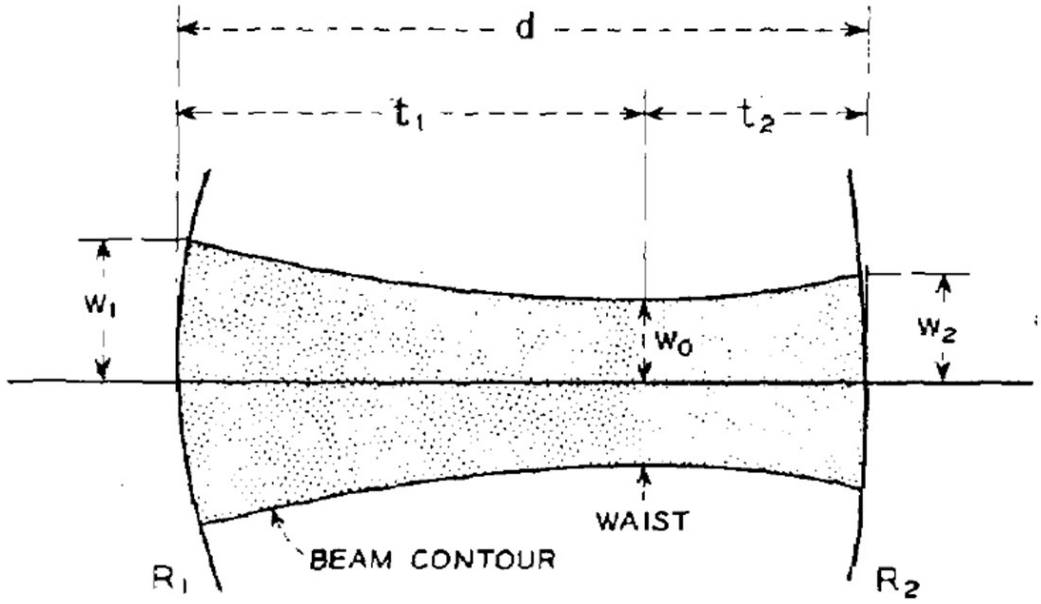

Figure 3: *Mode parameters of interest for a resonator with mirrors of unequal curvature (from Ref. [3]).*

mirrors of a stable resonator, $2w_1$ and $2w_2$, are given by

$$\begin{aligned} w_1^4 &= \left(\frac{\lambda R_1}{\pi}\right)^2 \frac{R_2-d}{R_1-d}\frac{d}{R_1+R_2-d}, \\ w_2^4 &= \left(\frac{\lambda R_2}{\pi}\right)^2 \frac{R_1-d}{R_2-d}\frac{d}{R_1+R_2-d}, \end{aligned} \tag{8}$$

where the radii of curvature of the mirrors are denoted R_1 and R_2. The diameter of the beam waist $2w_0$ is given by

$$w_0^4 = \left(\frac{\lambda}{\pi}\right)^4 \frac{d(R_1 - d)(R_2 - d)(R_1 + R_2 - d)}{(R_1 + R_2 - 2d)^2}. \tag{9}$$

The distances t_1 and t_2 between the waist and the mirrors, measured positive as shown in Fig. 3, are

$$t_1 = \frac{d(R_2 - d)}{R_1 + R_2 - 2d}, \quad \text{and} \quad t_2 = \frac{d(R_1 - d)}{R_1 + R_2 - 2d}. \tag{10}$$

The elements of the $ABCD$ matrix (see Ref. [3]) of this system can be used to calculate the mode parameters of the resonator. This yields for the corresponding beam radius w

$$w^2 = \left(\frac{2\lambda B}{\pi}\right) / \sqrt{4 - (A + D)^2}. \tag{11}$$

If z measures the distance along the optical axis from the position of the beam waist w_0, the Gaussian beam radius inside the cavity reads

$$w(z) = w_0 \sqrt{1 + \left(\frac{z}{z_R}\right)^2}, \tag{12}$$

with Rayleigh range $z_R = \frac{\pi w_0^2}{\lambda}$. Fig. 4 shows the beam radius distribution for the Advanced Virgo baseline design. The choice of beam waist affects the phase noise contribution. The noise

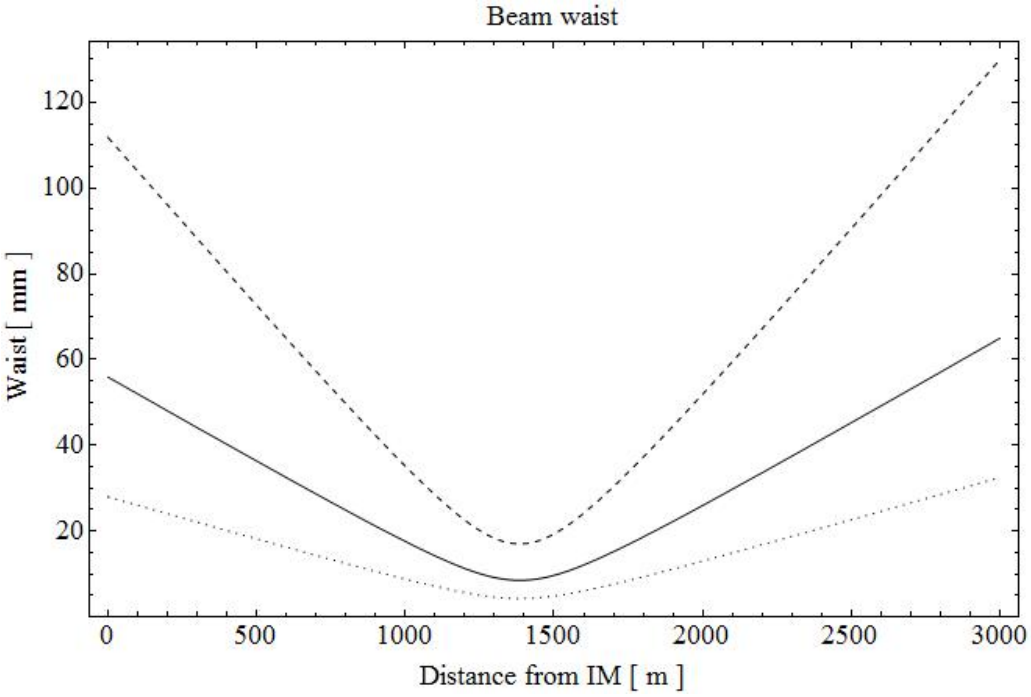

Figure 4: *Beam radius distribution for Advanced Virgo (solid curve). The dashed (dotted) curve shows the distribution for a factor two larger (smaller) beam waist.*

amplitude roughly increases as the square root of the waist. However, also the shape of the frequency spectrum is affected (a smaller beam radius leads to a harder noise spectrum).

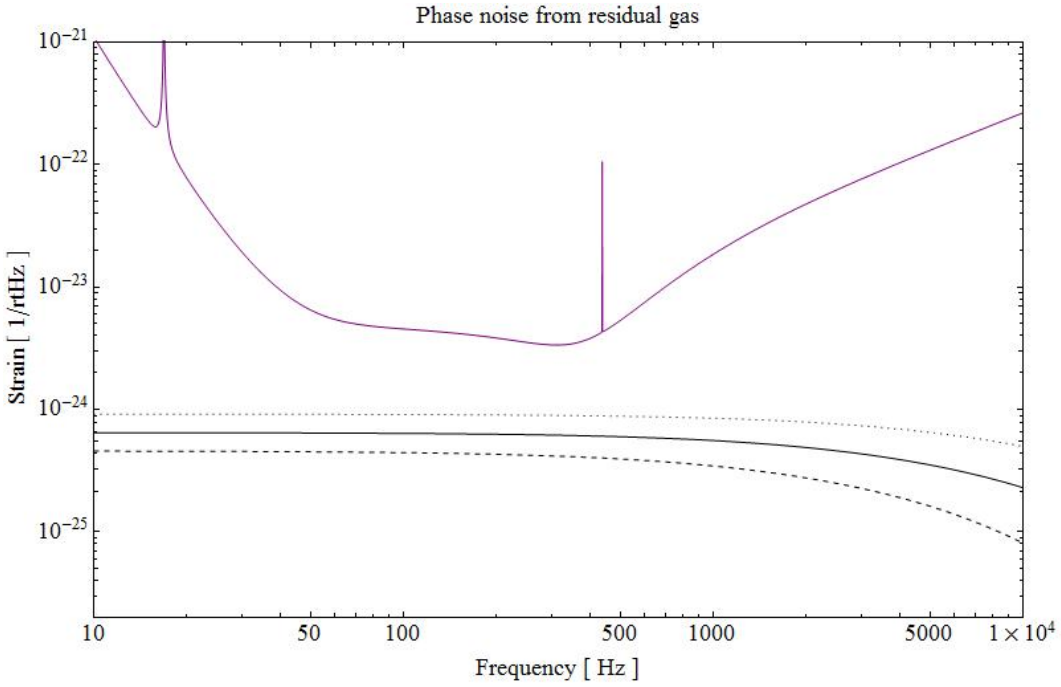

Figure 5: *Phase noise due to scattering of the laser beam from the residual gas. The different gas species have partial pressures given in Table 1.1. The purple curve represents the design sensitivity for Advanced Virgo. Note that the noise estimate deviates from the Virgo estimate.*

3 Results

Fig. 5 shows noise strain spectral amplitude densities due to the presence of nitrogen, water vapor, hydrogen and hydrocarbons in the interferometer arms. The figure reveales a weak dependence on the beam waist. A smaller beam size leads to a larger amplitude (the dependence roughly scales with the inverse square root of the waist). Furthermore, it is seen that a smaller waist leads to larger amplitudes at high frequencies. In order not to limit the strain sensitivity of Advanced Virgo, the partial pressure due to water vapor should be smaller than about $P_{\mathrm{H_2O}} \leq 10^{-9}$ mbar.

The previous expressions for the noise power spectrum can be used to determine the highest partial pressure that is compatible, for a given species, with a desired noise level. If we choose a particular species (*e.g.* water) as a reference, we obtain the simple expression

$$P_A = P_{\mathrm{H_2O}} \left(\frac{\alpha_{\mathrm{H_2O}}}{\alpha_A} \right)^2 \sqrt{\frac{m_{\mathrm{H_2O}}}{m_A}}, \tag{13}$$

which can be used to obtain estimates for the low frequency region.

4 Summary

This project note describes the scientific motivation for installing cryolinks in Advanced Virgo.

References

[1] '*Phase noise due to forward scattering*', R. Weiss, LIGO-T890025-00-R (1989).

[2] '*Measurement of Optical Path Fluctuations due to Residual Gas in the LIGO 40 Meter Interferometer*', Michael E. Zucker and Stanley E. Whitcomb, LIGO-P940008-00 (1994).

[3] '*Laser beams and resonators*', H. Kogelnik, T. Li, Applied Optics, Vol. 5, No. 10 (1966).